Title

Gas adsorption properties of ZSM-5 zeolites heated to extreme temperatures

Journal

Ceramics International, 42(14)

ISSN

0272-8842

Authors

Pérez-Page, María

Makel, James

Guan, Kelly

et al.

Publication Date

2016-11-01

DOI

10.1016/j.ceramint.2016.06.193

Peer reviewed

Ceramics International 42 (2016) 15423–15431

Contents lists available at ScienceDirect

Ceramics International

journal homepage: www.elsevier.com/locate/ceramint

Gas adsorption properties of ZSM-5 zeolites heated to extreme temperatures

María Pérez-Page [a], James Makel [a], Kelly Guan [b], Shenli Zhang [b], Joseph Tringe [c], Ricardo H.R. Castro [b], Pieter Stroeve [a,*]

[a] Department of Chemical Engineering, University of California Davis, Davis, CA 95616, United States
[b] Department of Materials Science and Engineering, University of California Davis, Davis, CA 95616, United States
[c] Lawrence Livermore National Laboratory, Livermore, CA, United States

ARTICLE INFO

Article history:
Received 29 April 2016
Received in revised form
27 June 2016
Accepted 28 June 2016
Available online 29 June 2016

Keywords:
Nanoporous solids
Surface area degradation
Pore collapse
Extreme temperatures
Gas adsorption
Helium adsorption

ABSTRACT

Zeolites are broadly useful catalysts and molecular sieve adsorbents for purification. In this work the thermal degradations of bare and platinum-loaded ZSM-5 was studied with the goal of understanding the behavior of nanoporous solids at extreme temperatures comparable to those present in nuclear fuels. Zeolites were heated in air and nitrogen at temperatures up to 1500 °C, and then characterized for thermal stability via X-ray diffraction (XRD) and for gas adsorption by the Brunauer-Emmett-Teller (BET) method. Scanning electron microscopy (SEM), differential scanning calorimetry (DSC) and thermal gravimetric analysis (TGA) were also employed. These results indicate zeolites are stable when heat-treated up to 800 °C and degrade slowly at higher temperatures. However, significant surface area degradation begins at 1025–1150 °C with an activation energy of 400 kJ/mole. At 1500 °C, gas adsorption measurements and SEM images show complete collapse of the porous structure. Critically for nuclear fuel applications, however, the zeolites still adsorb helium in significant quantities.

1. Introduction

There are many possible applications of nanoporous solids in extreme environments. For example, in a fission nuclear reaction, helium together with other fission product gases like xenon are generated [1,2]. These gases have a low solubility and diffusion in UO_2 [3] and above the saturation concentration they can create micro bubbles within the fuel leading to fuel swelling and increasing potential for release into the atmosphere. Materials designed to capture and retain these gases may be incorporated into the fuel, but they must survive high temperatures and high levels of radiation. If they are to remain functional during reprocessing operations, they must also react minimally with chemicals such as nitric acid and solvents [4]. The fuel in high-temperature reactors is operated at temperatures between 400 and 1200 °C [5], with a typical operation range of 750–950 °C [6]. However, fuel sintering processes are even higher, i.e. 1500 °C [7], though sintering times are much shorter in duration relative to fuel operation or storage. Microporous materials have found wide application in other areas such as catalysis [8,9], gas adsorption [10], biology [11] and many other fields. Additionally, nanoporous materials with good thermal stability are of interest for use in high-temperature environments for various applications [12,13]. In this work, we examine the feasibility of the nanoporous material zeolite for capturing fission product gases, especially helium. Zeolites are nanoporous crystalline aluminosilicates consisting of a complex framework of metal oxides. They have unique pore structures and large pore volumes between 40% and 50% of the crystal volume [14], finding use as catalysts [9,15,16], nuclear waste treatment [17,18] and even solar energy storage [19].

Previous research has demonstrated the utility of zeolites in high-temperature environments, such as catalyzed reduction on NO_x emissions from combustion to fossil fuels at temperature up to 600 °C [12] and catalytic conversion of methane to desired chemical products or liquid fuels [13]. These studies indicate the high thermal stability of zeolite, which derives from their specific porous structures and silicon/aluminum ratios [20–22], but they do not illuminate the upper limit for zeolite functionality, or provide insight into the mechanism by which zeolites ultimately degrade and fail.

ZSM-5 is a zeolite which consists of 10 membered ring openings [23,24]. The porous framework of ZSM-5 accounts for its high specific surface area and makes it an interesting material for gas adsorption [25]. Furthermore, compared to Y-type zeolites, ZSM-5 has an exceptionally high degree of thermal stability due to its high silicon/aluminum ratio and pore structure; it is therefore,

* Corresponding author.
E-mail address: pstroeve@ucdavis.edu (P. Stroeve).

http://dx.doi.org/10.1016/j.ceramint.2016.06.193
0272-8842/

potentially useful for processes involving elevated temperatures [20–22].

ZSM-5 zeolites can also be used in intimate contact with a hydrogenating component such as tungsten, vanadium, molybdenum, rhenium, nickel, cobalt, chromium, manganese, platinum or palladium [20]. Previously, it has been shown that the presence of rare earth cations in Y-type zeolites elevates the temperature at which the structure collapses [26].

In this work, zeolites are studied to determine if these materials are candidates for helium uptake after exposure to high temperatures. The physical properties of ZSM-5 zeolite and samples loaded with platinum are characterized as a function of temperature up to 1500 °C. To understand the structural evolution of the thermally treated zeolites, we employ X-ray diffraction (XRD), scanning electronic microscopy (SEM), thermogravimetric analysis (TGA), differential scanning calorimetry (DSC) and gas adsorption using the BET method. Comparing these results we can then establish an activation energy for the mechanism (or mechanisms) responsible for thermal degradation.

2. Experimental methodology

2.1. Materials

Commercial zeolite, NH_4-ZSM-5 (CBV2314), was obtained from Zeolite International (Conshohocken, PA). In addition, platinum loaded samples of ZSM-5 were prepared by Makel Engineering Inc. (Chico, CA). We chose the platinum loaded samples to determine if these had better thermal stability. The ZSM-5 ions in solution were exchanged with Pt ions in a 9–11 wt% aqueous platinum solution of tetra ammine platinum (II) chloride hydrate ($Pt(NH_3)_4Cl_2xH_2O$) obtained from Alfa Aesar. The mass ratio of zeolite to solution was 1:35. The sample loaded with Pt is referenced here as Pt-ZSM-5. The procedure for platinum loading consisted of four steps. First, the ZSM-5 zeolite was dried at 100 °C for 4 h. Second, the dried zeolite was weighed and then allowed to undergo ion exchange with the appropriate amount of aqueous platinum solution in a beaker mixed by a magnetic stir bar for 24 h at room temperature. Third, the resulting powder was filtered, rinsed with distilled water and calcined in air at 300 °C for 3 h. Finally, the calcined product was reduced in a 10% hydrogen gas (balance nitrogen) flowing (500 sccm) at 450 °C for 6 h.

2.2. X-ray diffraction

A Bruker-AXS D8 Advance diffractometer (Bruker-AXS, Inc.) operating at an accelerating voltage of 40 kV and an emission current of 40 mA with CuKα (λ=0.15406 nm) was used to collect XRD powder patterns for the samples. XRD patterns were collected between 2θ angles of 5–60° with a step size of 0.02°. Samples were mounted on zero-background holders.

2.3. Scanning electron microscopy (SEM) and energy dispersive X-Ray spectroscopy (EDS)

The zeolites were analyzed using SEM/EDS to determine particle size and to determine Si/Al atomic ratios. To facilitate SEM characterization, the zeolite powder was lightly ground and dusted onto double-sided carbon tape, then sputter-coated with Au-Pd for two minutes to improve the conductivity. The coating was performed with a plasma sputtering coater Denton Vacuum Desk II. Images were captured at different magnifications with a Philips XL30 SFEG SEM at 5 kW using a thermo-luminescent detector (TLD) detector. EDS measurements were taken at 5 kW electron beam accelerating power.

2.4. Adsorption experiments

Gas adsorption measurements commonly determine the adsorption isotherm, the surface area and pore size distribution of many porous materials, such as industrial adsorbents, catalysts, pigments, and ceramics [27,28]. To determinate the adsorption isotherm, the surface area and the pore size, experiments were conducted with a Micromeritics Gemini VII 2390 surface area analyzer. Samples (15–20 mg) were pretreated to remove adsorbed contaminants from atmospheric exposure to air by degassing under vacuum at 400 °C for at least 12 h with a Micromeritics VacPrep 061.

The surface area and pore size distribution were determined using nitrogen as the adsorptive gas. Samples were cooled, under vacuum, at 77 K. Then nitrogen was introduced to the sample in controlled, incremental amounts. After each application of the adsorptive gas, the pressure was allowed to equilibrate and the quantity of gas adsorbed on the sample was calculated from the measured pressure. The gas volume adsorbed at each pressure at constant temperature gives the adsorption isotherm. The method of Brunauer, Emmett, and Teller (BET) was employed to determine the surface area [29], using a Micromeretics Gemini VII surface area analyzer. In addition to nitrogen adsorption at 77 K, the adsorption of nitrogen and the noble gases helium and argon was measured at room temperature, 23 °C.

2.5. Differential scanning calorimetry and thermogravimetric analysis

The thermal stability of the zeolites was studied using differential scanning calorimetry/thermal gravimetric analysis (DSC/TGA). DSC and TGA analyses were acquired simultaneously on a Setaram Setsys Evolution 1750 DSC/TGA Analyzer. All samples were run as powders in alumina crucibles under synthetic air atmosphere (1 atm) at a heating rate of 10 K/min from room temperature up to 1500 °C. The temperature was then decreased to room temperature at a rate of 20 K/min.

2.6. Heat treatment

Zeolite samples were treated at high temperatures to observe and characterize their thermal degradation. Two different heat treatments were conducted. First, both zeolites, ZSM-5 and Pt-ZSM-5, were each heated to 800, 1200 and 1500 °C. These temperatures were selected from our DSC/TGA results, as reported below in Section 3.2. Samples were heated in the presence of air (1 atm) at a rate of 10 °C/min to the target temperature using the Setaram Setsys Evolution 1750 DSC/TGA Analyzer. The airflow rate was 20 mL/min. Once the samples achieved the desired temperature, the samples were cooled at a rate of 20 °C /min to room temperature.

A second heat treatment was used to develop a model for the degradation of the Pt-ZSM-5. To observe exclusively thermal surface area degradation, the heat treatment was performed in a presence of nitrogen ambient. This avoids any chemical reactions such as oxidation that would occur in air. Zeolite samples were exposed to temperatures of 950, 1000, 1050, 1100 and 1150 °C under a nitrogen atmosphere for 2 h. The temperature was increased at a constant rate of 10 °C/min to 800 °C and at a constant rate of 5 °C/min above 800 °C. The samples were heated in an alumina tube furnace GSL 1700X-60 from MTI Corporation.

3. Results and discussions

3.1. Characterization of zeolites before heat-treatment

Fig. 1 shows the X-ray diffraction (XRD) patterns of the zeolites. The zeolites have the typical patterns of the ZSM-5 structure [30–32], in agreement with Powder Diffraction File No #44–0024, with 2θ at 14.8°, 23.27°, 23.86°, 24.58°, 29.46°, 30.31°, and 45.63° corresponding to the major peaks of (301), (501), (422), (313), (532), (616), and (1000). The diffraction pattern of Pt-ZSM-5 shows that the crystal structure of the zeolite is maintained after platinum loading. The XRD reflection of Pt particles is observed in a new peak which does not exist for the ZSM-5 zeolite at 2θ = 39.98°. This peak corresponds to (111) for platinum [Powder Diffraction File No #70–2431] [33,34]. Since metallic Pt has an atomic diameter of 2.7 Å, large Pt crystals cannot form inside the channels. However, Pt crystals could form on the outside surface of the zeolite particles.

Fig. 2 shows representative SEM images for the ZSM-5 zeolite sample. Particles are irregularly shaped, with smaller particles having largest dimension of ~100 nm; larger particles have largest dimensions of a few hundred nm. From the EDS results shown in the Table 1, the zeolites are primarily composed of Si and Al, as expected. The Si/Al atomic ratio is 22 (calculated from the EDS results) for ZSM-5, close to the ratio of 23 reported by Zeolyst International.

The nitrogen adsorption isotherms of zeolites ZSM-5 and Pt-ZSM-5 are shown in Fig. 3. The features of the isotherms indicate only filling of micropores and no presence of mesopores. The isotherms show high nitrogen uptake at low relative pressure and a plateau at high relative pressure, typical from the microporous materials. The sub-step observed around P/Po = 0.2 in the isotherm is a typical feature of MFI type zeolites and is associated with a fluid-to-solid-like phase transition of the adsorbed nitrogen in microporous network [27]. The two isotherms are similar, however the ZSM-5 isotherm shows a higher quantity of adsorbed nitrogen. This may be due to a partial blockage of nitrogen by Pt atomic clusters or due to Pt atoms occupying adsorption sites inside the zeolite channels.

Adsorption isotherm data can be used for characterizing the gas adsorption properties of porous materials [31,32,35,36] and are used to obtain specific surface areas. The use of the calculated surface area is controversial for microporous media [37–40], however the practice is widespread. Here, we use the specific surface area solely as comparative measure for analyzing the effects of thermal treatments of the zeolites. The surface areas obtained are given in Table 2 and ZSM-5 gives the highest specific surface area.

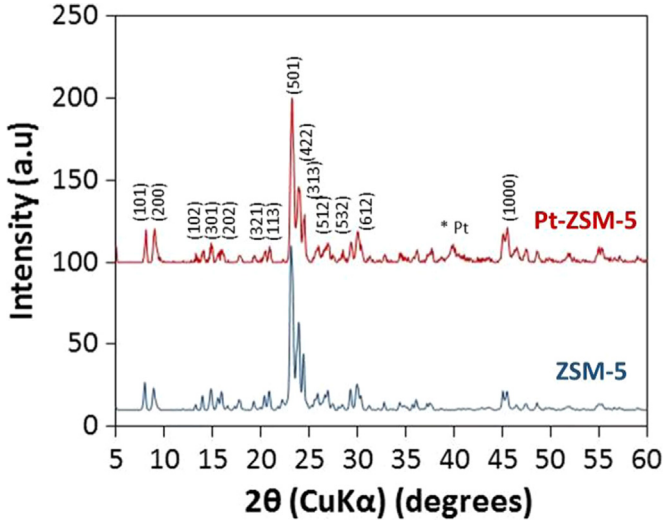

Fig. 1. XRD patterns of ZSM-5 and Pt-ZSM-5. The location of the Pt peak is indicated on the figure.

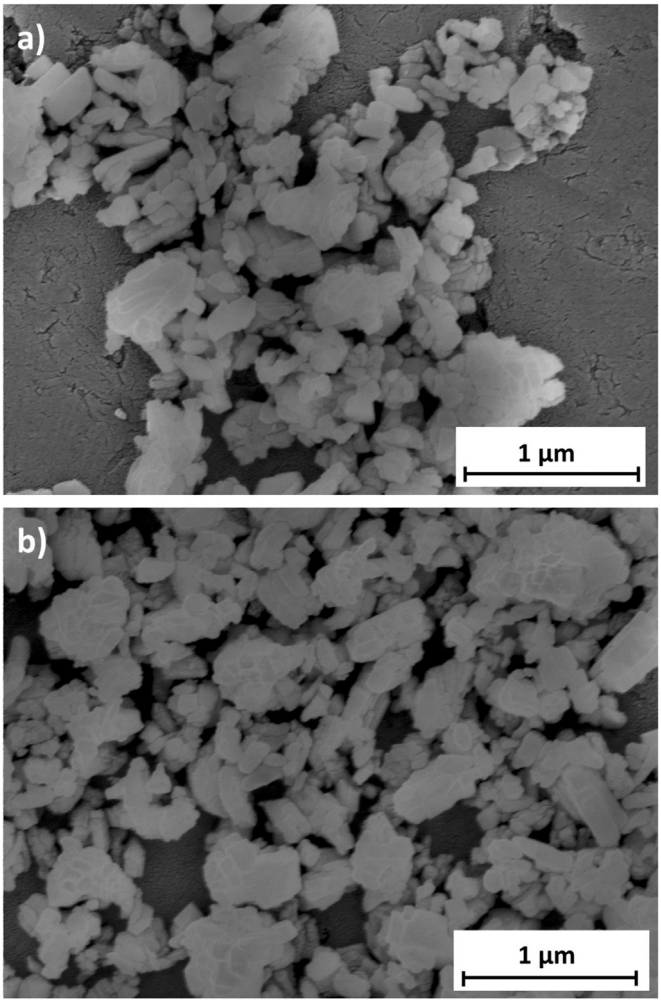

Fig. 2. Zeolite ZSM-5 SEM pictures take at 5 kV and 65 Kx.

Table 1
EDS results of ZSM-5.

Element	ZSM-5
O (at%)	47.4 ± 10.59
Al (at%)	2.24 ± 0.66
Si (at%)	50.36 ± 14.05

3.2. Thermal degradation of zeolites

Thermal stability is the resistance that a material has to decomposition at high temperatures. To study the thermal stability of zeolites, TGA and DSC were carried out on the zeolite samples following the protocol described in the experimental methodology (Section 2.6). Figs. 4 and 5 show the TGA/DSC profiles of the zeolites in air up to 1500 °C. One can observe that there is an endothermic peak between 100 and 250 °C, which is due to loss of water of hydration from the pores. From the TG profile in this range of temperatures, the weight decreases up to 250 °C, then, the loss of weight is more gradual up to 1000 °C and then is stable from 1000 to 1500 °C.

The total lost mass is 7.5% for ZSM-5 and 6.5% for Pt-ZSM-5 over the total temperature range. About 75% of the total weight loss

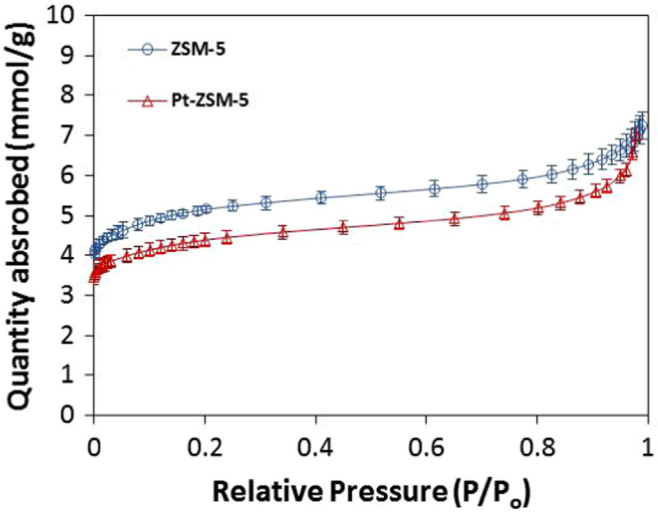

Fig. 3. Nitrogen adsorption isotherms of ZSM-5 and Pt-ZSM-5 at 77 K.

Table 2
Specific surface area for ZSM-5, Pt-ZSM-5.

Zeolite	Specific surface area (m^2/g)
ZSM-5	410 ± 5
Pt-ZSM-5	386 ± 1

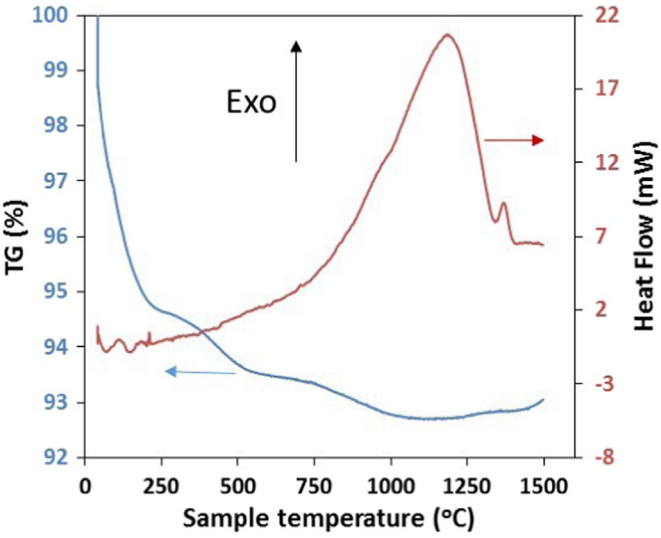

Fig. 4. TGA/DSC profiles of ZMS-5 zeolite in air to 1500 °C.

occurs from 0 and 250 °C due to removal of the water of hydration [30,41,42]. Fig. 4 shows a large exothermic peak centered at about 1200 °C for the ZSM-5 zeolite, which is likely attributed to a phase transition since at that point the porous structure of zeolite has collapsed [20]. Note that there is not a corresponding change in mass, consistent with crystallization. A small shoulder is observed at about 1000 °C, suggesting the process occurs in two steps. Fig. 5 clearly shows two smaller exothermic peaks for Pt-ZMS-5, the smallest at around 920 °C, probably due to the local collapse of the porous structure, followed by a larger peak at 1200 °C due to crystallization. Both peaks at 1200 °C in Figs. 4 and 5 are attributed to crystallization of a new phase, likely cristobalite.

Comparing Figs. 4 and 5 the exothermal heat flow of ZSM-5 is larger than that of Pt-ZSM-5. The ZSM-5 exothermic heat flow begins with the shoulder at about 500 °C and then begins to grow

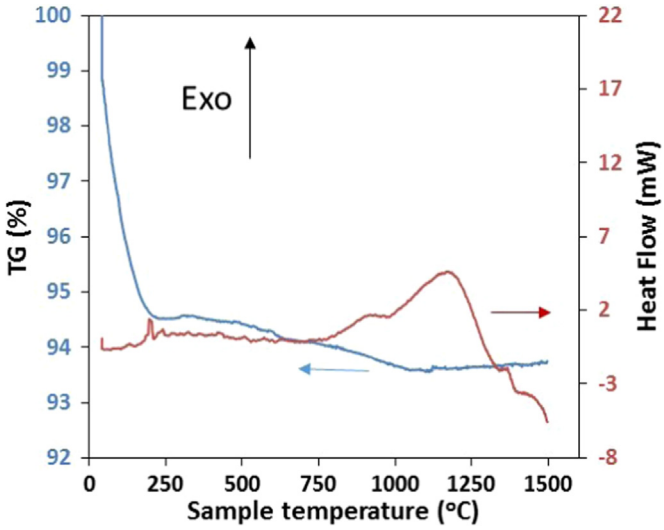

Fig. 5. TGA/DSC profiles of Pt-ZMS-5 zeolite in air to 1500 °C.

at about 750 °C while in the Pt-loaded zeolite the second exothermic peak begins at 950 °C. This small difference between the thermal signature of the modified zeolite versus the original zeolite may be due to Pt hindering diffusion of the components, retarding phase transition kinetics and may indicate a somewhat improved thermal stability compared to ZSM-5.

It has been reported that ZSM-5 is thermally stable to 930 °C [20,21]. Since the DSC/TGA results indicate changes in the structure starting around 920 °C, XRD experiments were performed to determine if there are phase transitions for the zeolites when they are heated up to 1500 °C. Figs. 6 and 7 show the XRD patterns for the zeolites ZSM-5 and Pt-ZSM-5 heated to 800, 1200 and 1500 °C, respectively. The XRD results show that the intensities of the main spectrum peaks, (501), (422), and (313) (Fig. 1) decrease from 800 to 1200 °C. However, Fig. 7 shows that the peak that corresponds to platinum (2θ at about 40°) increases, and a new peak at 46.37° appears for temperatures between 800 and 1200 °C [33,34]. This new peak also corresponds to (200) planes and suggests that Pt is starting to coarsen into larger particles as the structure crystallizes.

When the thermal treatment is at 1500 °C, the typical peaks of ZSM-5 disappear and new ones, corresponding to a cristobalite-like structure (Powder Diffraction File No #77–1316), appear. Note

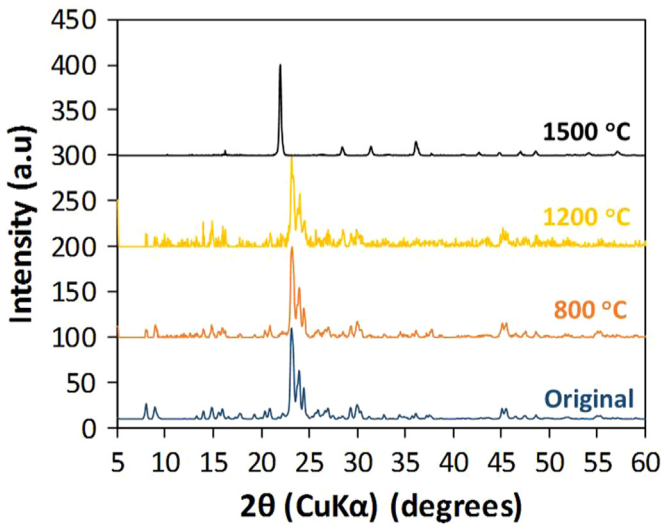

Fig. 6. XRD patterns at room temperature for ZSM-5 heated to 800, 1200, or 1500 °C compared with the original ZSM-5 sample at room temperature.

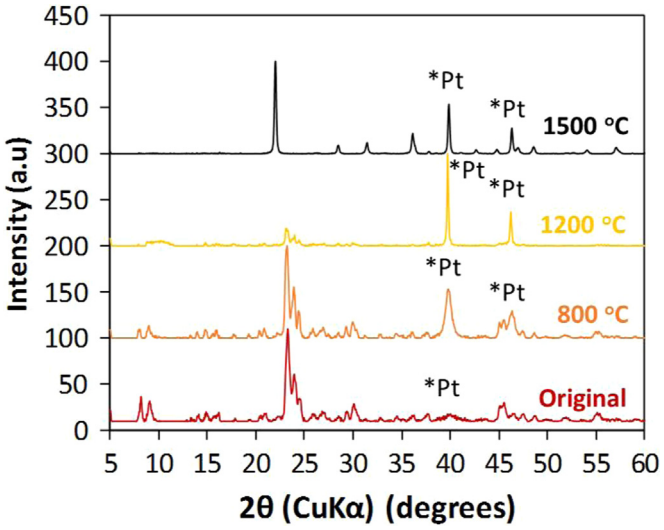

Fig. 7. XRD patterns at room temperature for Pt-ZSM- heated to 800, 1200, and 1500 °C compared with the original Pt-ZSM-5 sample at room temperature.

that cristobalite is composed of SiO_2; however the zeolite is composed also of alumina. In order to determine if the alumina is still present in the zeolites after the heat treatment at 1500 °C, EDS experiments were performed. Curiously, at 1200 °C the ZSM-5 appears to still retain a diffraction pattern similar to the original, but Pt-ZSM-5 has significant changes at 1200 °C.

Table 3 shows the Si/Al ratio of the two zeolites after the heat treatment at 1500 °C.

Si/Al ratios obtained for ZSM-5 and Pt-ZSM-5 after the heat treatment are slightly higher than the Si/Al ratios obtained in the zeolites before the heat treatments (see Section 3.1 and Table 3) indicating only a small loss of alumina. Thus the EDS results show that alumina is still present in the zeolites after the heat treatment and the results are supported by the DSC/TGA data, which only show a small mass reduction. The XRD spectra at 1500 °C show a cristobalite structure which is composed only of SiO_2, which suggests that alumina may have changed into a completely amorphous structure which cannot be observed by XRD.

Fig. 8 shows SEM pictures of different zones of the ZSM-5 sample heat treated up to 1500 °C. Images were taken at different magnifications. Individual particles of ZSM-5 can be observed in Fig. 8(b) and (d). These particles are similar to the particles that can be observed in the SEM images of ZSM-5 without any heat treatment (Fig. 2). However, other zones of the samples show that particles are more agglomerated and the images show bigger particles than in the original sample. This means that during the heat treatment, individual particles were sintered together as shown in Fig. 8(c) via liquid phase sintering, commonly present in aluminosilicate systems.

3.3. Effect of the temperature in the nitrogen adsorption isotherms and surface area at 77 K

The decomposition of the zeolite samples has been characterized by gas adsorption measurements. Temperatures were selected corresponding to the peaks on the DSC profiles, i.e., 800 °C and 1200 °C. In addition, zeolites samples were heated to 1500 °C. The heat treatment was carried out in air as described by the procedure given in the experimental section. The adsorptive properties and the composition of each zeolite are reported below.

Table 3
Si/Al atomic ratios of zeolites after heat treatment at 1500 °C compared with the ratios obtained for the zeolites before the heat treatment.

Zeolite	Si/Al ratio (1500 °C)	Si/Al ratio (as made)
ZSM-5	13.8 ± 0.4	11.5 ± 0.3
Pt-ZSM-5	14.4 ± 0.3	12.4 ± 0.6

The nitrogen adsorption isotherms of the zeolites after heat treatment in air to 800 and 1200 °C, respectively, are shown in Figs. 9 and 10. The error bars, based on two standard deviations, indicate that the gas adsorption properties of ZSM-5 and Pt-ZSM-5 are similar within the margin of error. A small difference is observed in the Pt-ZSM-5 isotherm. Interestingly, the adsorption isotherms at 800 °C are nearly identical to those observed for the untreated zeolites shown in Fig. 3. These results indicate that the start of the exothermic heat flows observed by DSC at 750 and 800 °C (see Figs. 4 and 5) do not result in significant changes in the gas adsorption properties and therefore the pore structures in the zeolites. However, comparisons between the isotherms for the zeolites heat-treated to 800 °C (Fig. 9) with the isotherms for the zeolites heat-treated to 1200 °C (Fig. 10) show a drastic reduction of the gas adsorption properties for the samples treated to 1200 °C. The exothermic peak at 1200 °C (Figs. 4 and 5) and the results in Fig. 10 indicate significant changes in pore structure occurred in the pore volumes. These changes are consistent with the XRD results.

Table 4 shows the specific surface areas of ZSM-5 and Pt-ZSM-5 at different temperatures. The surface areas decrease when the heat treatment temperature increases. The specific surface areas of the samples at 1500 °C are lowest for each zeolite, indicating that the porosity of the sample is low, corresponding to a structural collapse, in agreement with the previous results with DSC and the nitrogen adsorption isotherms.

The pore size distribution and the maximum pore volume measured at $P/P_o = 0.989$ for both zeolites, ZSM-5 and Pt-ZSM-5, heat treated to different temperatures are represented in Table 5. The pore size distribution based on the nitrogen adsorption isotherms can be derived from several methods. Methods are based on the micropore filling theory and on the interaction potential between adsorbate and adsorbent such as the Horvath and Kawazoe (H-K) model, which is a simple and popular model for evaluating pore size distribution of microporous materials [16]. This technique is often used for the determination of the pore size distribution in many microporous adsorbents such as activated carbon or zeolites.

The pore size distribution and the maximum pore volume remain about the same when the temperature increases to 800 °C. At 1200 °C the values are difficult to measure because they are small and have large standard deviations.

3.4. Comparison of the adsorption of helium, argon and nitrogen at room temperature

Crystallization of zeolite at high temperatures decreases pore volume, and consequently, adsorbed nitrogen. Furthermore, a constriction of the pores limits the entrance of nitrogen into the pores. However, smaller gas atoms such as helium, could still enter if inter-atomic spacing allows. Helium has a kinetic diameter of 2.6 Å [43], while the unit cell of cristobalite, the polymorph of silica observed after high-temperature treatment of zeolite, has a smallest lattice constant dimension of 4.97 Å [44].

The helium condensation temperature is 4 K. This temperature presents a significant barrier to performing gas adsorption measurements at the condensation temperature. To compare the adsorption of different gases at the same conditions, adsorption studies at room temperature using nitrogen, helium and argon were performed. Figs. 11–14 show the helium, argon, and nitrogen isotherms at room temperature of Pt-ZSM-5 without heat-treatment and with heat treatments.

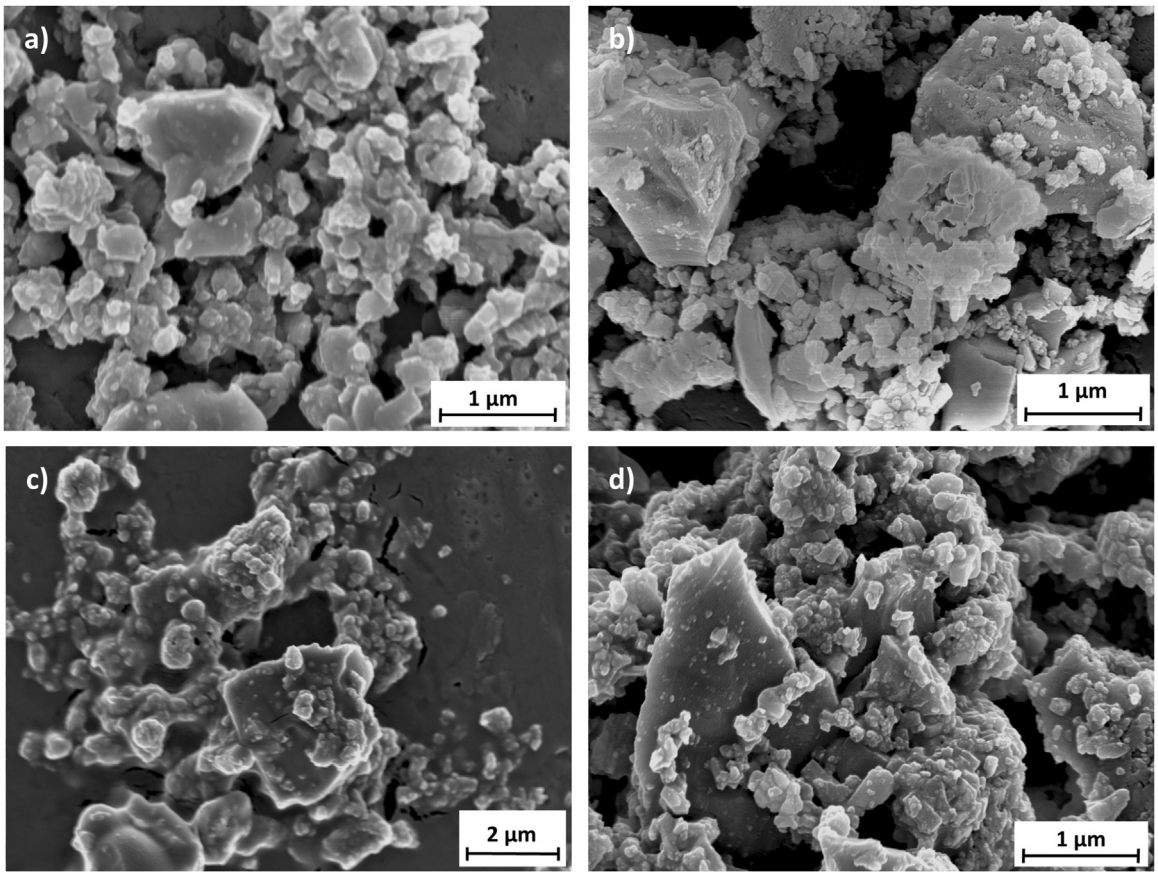

Fig. 8. Zeolite ZSM-5 heat treated at 1500 °C pictures taken at 5 kW at different magnifications. a), b) and d) images taken at 25 Kx is 1 µm. Image c) taken at 10 Kx, the bar is 2 µm.

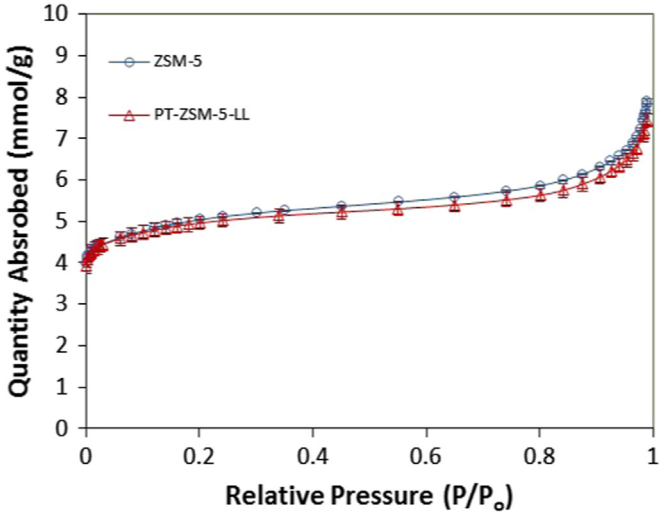

Fig. 9. Nitrogen adsorption isotherms at 77 K for ZSM-5 and Pt-ZSM-5 heat-treated to 800 °C.

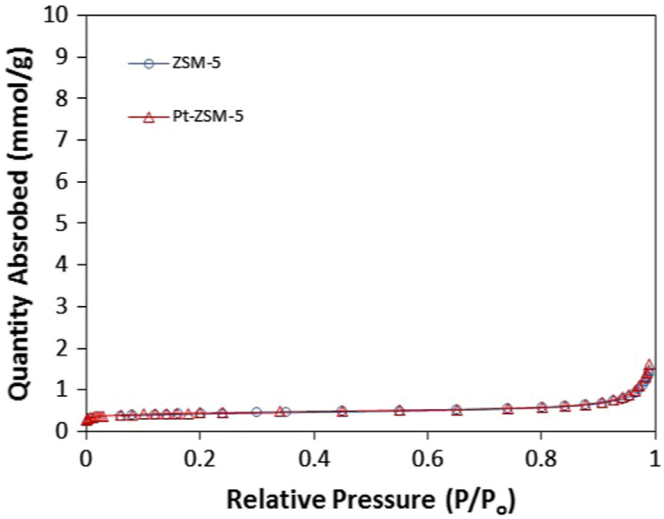

Fig. 10. Nitrogen adsorption isotherms at 77 K for ZSM-5 and Pt-ZSM-5 heat-treated to 1200 °C.

For the original Pt-ZSM-5, the three isotherms are shown in Fig. 11. There is virtually no difference when the relative pressure approaches 1. However, at lower relative pressures the quantity of adsorbed helium is considerably higher than that of argon and nitrogen.

Figs. 12–14 show the isotherms for helium, nitrogen and argon at room temperature for Pt-ZSM-5 heated to 800, 1200 and 1500 °C, respectively. One can observe that for the three temperatures the quantity of adsorbed helium is considerably higher than the quantities for argon and nitrogen. Argon has the lowest adsorption. Further, for the zeolite heated up to 800 °C, the quantity adsorbed is higher than for the original zeolite (Fig. 11). The difference between the isotherms becomes larger when the zeolite is heated to 1500 °C, as seen in Fig. 14.

For the zeolite samples heated to 1500 °C, the structure is different than at the lower temperatures: a cristobalite-type structure has formed, the pores are completely collapsed and the adsorption properties are decreased. However, the zeolites can still adsorb helium after the heat treatment at 1500 °C. Helium is the

Table 4
Surface areas of ZSM-5, and Pt-ZSM-5 heated to different temperatures. At 1500 °C, the specific surface areas of ZSM-5 and Pt-ZSM-5 are not measurable.

Temperature (°C)	Specific surface area (m^2/g)	
	ZSM-5	Pt-ZSM-5
Room temperature	410 ± 5	386 ± 1
800	389 ± 3	399 ± 1
1200	35 ± 3	34 ± 5
1500	–	–

smallest molecule, so when the pores collapse, helium still penetrates the densified material, as allowed by inter-atomic spacing.

3.5. Degradation model at high temperatures

The degradation of zeolite Pt-ZSM-5 in nitrogen at high temperatures was studied. Five samples were held for two hours at one of the following five temperatures: 950, 1000, 1050, 1100 and 1150 °C. Heating rates for this thermal treatment are described in Section 2.6. BET adsorption studies at 77 K were carried out on each sample with the method described in the experimental methodology.

Fig. 15 shows the relation between the apparent specific surface area and the treatment temperature. Collapse of the pore structure and the degradation of the specific surface area start at about 1025 and is complete at 1150 °C. The behavior is similar to the results discussed previously for samples heated in air. At lower temperatures the change in the specific surface area is not significant, but the most significant change in the surface area is observed in the temperature range of 1025–1100 °C, which corresponds to the collapse of the porous structure of ZSM-5. This behavior is consistent with the results for the DSC/TGA and adsorption measurements presented previously.

The temperature dependence of the rate of decay for the specific surface area can be modeled as an Arrhenius process as shown in Eq (1) [45]. The time derivative in Eq. (1) was approximated by dividing the change in specific surface area by the holding time of two hours described previously.

$$\frac{dA_{sp}}{dt} = k(T) = C \bullet e^{-\frac{E_A}{R \bullet T}} \quad (1)$$

Eq. (1) was linearized and fit via sum of least squares regression to find E_A and C. The best fit gave an activation energy, E_A, of 402 kJ/mole with C equal to $-1.399 \cdot 1014\ m^2/(g\ s)$. Simple integration of Eq. (1) results in Eq. (2) which can be used to predict the apparent specific surface area for a Pt-ZSM-5 sample exposed to temperature, T, and time, t, within a range close to those described. Here, A_{sp0} is the specific surface area of a sample that has not experienced decay.

$$A_{sp}(t, T) = A_{sp0} + (C \bullet t) e^{-\frac{E_A}{(R \bullet T)}} \bullet \quad (2)$$

Experimental values of the surface area and the predicted values using Eq. (2) are displayed in Fig. 15. A good fit is obtained at intermediate temperatures, which is the region where the specific surface area degrades significantly. The fit fails at higher temperatures likely because pore collapse drastically changes the geometry of the surface being interrogated by gas molecules employed for the area measurement.

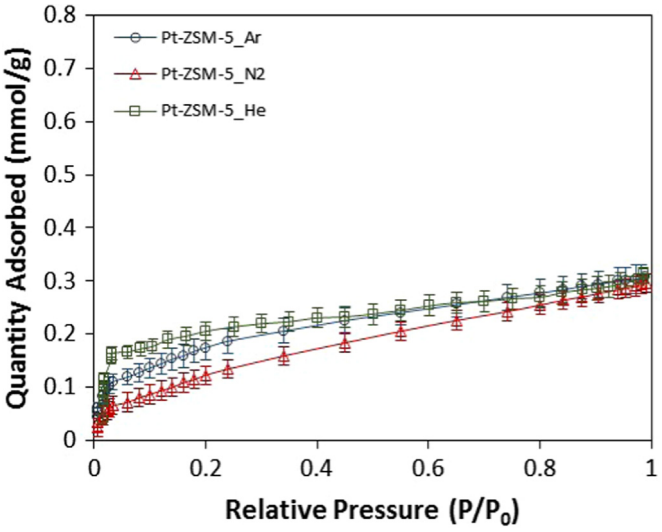

Fig. 11. Argon, nitrogen and helium adsorption isotherms at room temperature for Pt-ZSM-5, not heat-treated.

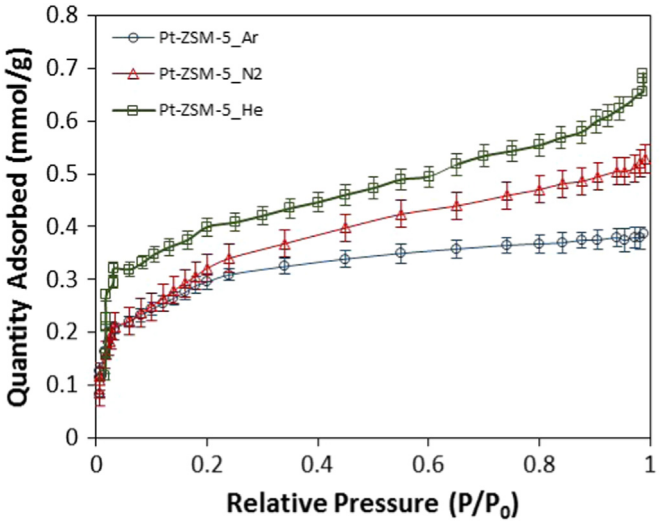

Fig. 12. Argon, nitrogen and helium adsorption isotherms at room temperature of Pt-ZSM-5 heated to 800 °C.

4. Conclusion

The gas adsorption, chemical and structural properties of commercial zeolite ZSM-5 and a Pt loaded variant (Pt-ZSM-5) have

Table 5
Pore size distribution and maximum pore volume of ZSM-5 and Pt-ZSM-5 heated to different temperatures. At 1200 and 1500 °C, the values of ZSM-5 and Pt-ZSM-5 too small or lead to large standard deviations.

Temperature (°C)	Pore size distribution (nm)		Maximum pore volume at $P/P_o = 0.989$ (cm^3/g)	
	ZSM-5	Pt-ZSM-5	ZSM-5	Pt-ZSM-5
Room temperature	0.64 ± 0.26	0.74 ± 0.3	0.25 ± 0.003	0.246 ± 0.003
800	0.72 ± 0.4	0.73 ± 0.5	0.266 ± 0.006	0.255 ± 0.007
1200	–	–	0.05 ± 0.005	0.055 ± 0.008
1500	–	–	–	–

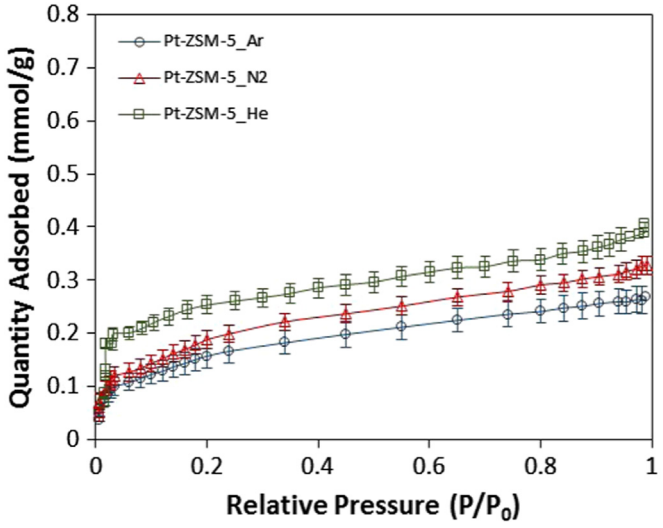

Fig. 13. Argon, nitrogen and helium adsorption isotherms at room temperature of Pt-ZSM-5 heated to 1200 °C.

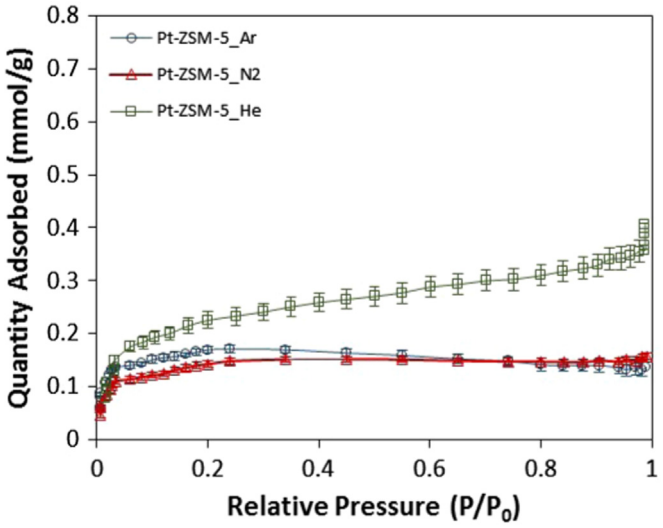

Fig. 14. Argon, nitrogen and helium adsorption isotherms at room temperature of Pt-ZSM-5 heated to 1500 °C.

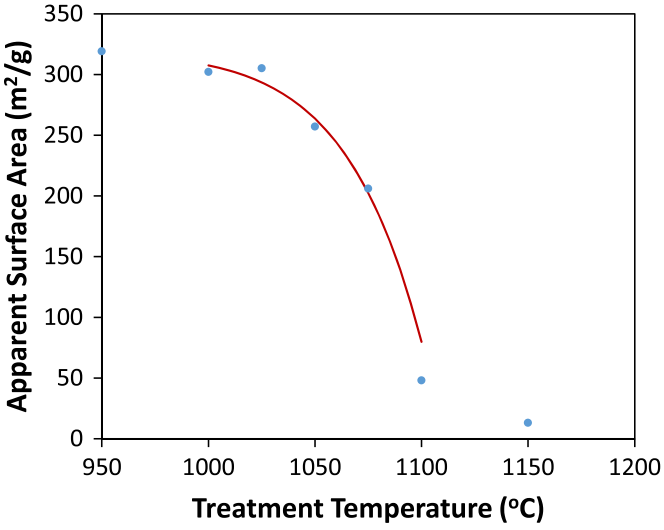

Fig. 15. Relationship of the apparent specific surface area with the temperature of Pt-ZMS-5.

been observed as a function of temperature. These materials have an specific surface area between 300 and 400 m^2/g, as determined by nitrogen adsorption using the BET method. Measured XRD spectra are typical for ZSM-5 zeolites. ZSM-5 is chemically and structurally stable in air up to 750 °C, while Pt-ZSM-5 is stable to about 800 °C. Above these temperatures the porous framework of the zeolites begins to degrade.

Degradation of zeolites at temperatures above 800 °C was studied: samples were heated up to 1500 °C. BET experiments were carried out at room temperature to determine the adsorptive properties of the heat treated zeolites. The specific surface area decreases with increasing treatment temperature. Nitrogen adsorption data indicate that heating samples to 1500 °C causes the porous network to collapse. XRD patterns show that at high temperature ZSM-5 transitions to cristobalite. Only small differences are observed between the ZSM-5 and the Pt-ZSM-5.

Adsorption studies with helium, argon and nitrogen at room temperatures were performed with the zeolites Pt-ZSM-5 treated at 800, 1200, and 1500 °C. The results show that the quantity of adsorbed helium is higher than nitrogen and argon, and that argon adsorbs the least. When the temperature increases, the pores collapse and impede access to the interior structure. Importantly, the small helium atoms retain access to the densified material.

An Arrhenius model was developed to characterize the degradation of zeolite in nitrogen at high temperatures. Collapse of the pore structure and the degradation of the specific surface area start at about 1000 °C and is complete at 1150 °C. The decay of the apparent specific area depends on the temperature and this dependence follows the Arrhenius equation. The relationship between the surface area and the treatment temperature permits prediction of the specific surface area of Pt loaded ZSM-5 sample as a function of temperature.

This work has useful implications for nuclear fuel applications where gas capture at high temperatures may be needed. The zeolites appear to retain measureable helium incorporation even after being processed at 1500 °C, in the temperature range of UO_2 fuel sintering. Nanostructured zeolites particles, appropriately distributed within fuel pellets, may therefore provide utility for helium sequestration in operational reactors. Although additional studies are needed to establish the full potential of this approach, the data are encouraging and merit further consideration for this application.

Acknowledgements

This material is based upon work supported by the Department of Energy [National Nuclear Security Administration] under Award Number DE-NE0000704.

References

[1] F. Rouquerol, J. Rouquerol, K. Sing (Eds.), Adsorption by Powders and Porous Solids: Principles, Methodology and Applications, Academic Press, London, 1999.
[2] I. Zacharie, S. Lansiart, P. Combette, M. Trotabas, M. Coster, M. Groos, Microstructural analysis and modelling of intergranular swelling of an irradiated UO2 fuel treated at high temperature, J. Nucl. Mater. 255 (1998) 92–104.
[3] D. Roudil, X. Deschanels, P. Trocellier, C. Jegou, S. Peuget, J.M. Bart, Helium thermal diffusion in a uranium dioxide matrix (vol 325, pg 148, 2004), J. Nucl. Mater. 327 (2004) 226.
[4] M. Benedict, T.H. Pigford, H.W. Levi, Nuclear Chemical Engineering, Mcgraw-Hill, 1981.
[5] C. Ferry, J.-P. Piron, A. Ambard, Effect of helium on the microstructure of spent fuel in a repository: an operational approach, J. Nucl. Mater. 407 (2010) 100–109.
[6] World Nuclear Association Nuclear Fuel Fabrication.

[7] P. Balakrishna, C.K. Asnani, R. Kartha, K. Ramachandran, K.S. Babu, V. Ravichandran, et al., Uranium dioxide powder preparation, pressing, and sintering for optimum yield, Nucl. Technol. 127 (1999) 375–381.
[8] N.Z. Logar, V. Kaucic, Nanoporous materials: from catalysis and hydrogen storage to wastewater treatment, Acta Chim. Slov. 53 (2006) 117.
[9] CN. Satterfield, Heterogeneous Catalysis in Industrial Practive, 2nd ed.,1994.
[10] R.E. Morris, P.S. Wheatley, Gas storage in nanoporous materials, Angew. Chem. Int. Ed. 47 (2008) 4966–4981.
[11] S.P. Adiga, C. Jin, L.A. Curtiss, N.A. Monteiro-Riviere, R.J. Narayan, Nanoporous membranes for medical and biological applications, Wiley Interdiscip. Rev: Nanomed. Nanobiotechnol. 1 (2009) 568–581.
[12] J.W. Byrne, J.M. Chen, B.K. Speronello, Selective catalytic reduction of NOx using zeolitic catalysts for high temperature applications, Catal. Today 13 (1992) 33–42.
[13] L. Wang, L. Tao, M. Xie, G. Xu, J. Huang, Y. Xu, Dehydrogenation and aromatization of methane under non-oxidizing conditions, Catal. Lett. 21 (1993) 35–41.
[14] J.C.M. Muller, G. Hakvoort, JC. Jansen, DSC and TG study of water adosorption and desorption on zeolite NaA powder and attached as layer on metal, J. Therm. Anal. Calorim. 53 (1998) 449–466.
[15] S.M. Csicsery, Shape-selective catalysis in zeolites, Zeolites 4 (1984) 202–213.
[16] X. Du, E. Wu, Porosity of microporous zeolites A, X and ZSM-5 studied by small angle X-ray scattering and nitrogen adsorption, J. Phys. Chem. Solids 68 (2007) 1692–1699.
[17] A. Dyer, A.S.A. Gawad, M. Mikhail, H. Enamy, M. Afshang, The natural zeolite, laumontite, as a potential material for the treatment of aqueous nuclear wastes. Journal of Radioanalytical and Nuclear, Chem. Lett. 154 (1991) 265–276.
[18] A. Dyer, D. Keir, Nuclear waste treatment by Zeolites, Zeolites 4 (1984) 215–217.
[19] R.A. Shigeishi, C.H. Langford, B.R. Hollebone, Solar-energy storage using chemical-potential changes associated with drying of zeolites, Sol. Energy 23 (1979) 489–495.
[20] Robert J. argauer K, Md., George R., Landolt, N.J., Audobon, Assignors to Mobil Oil Corporation, crystalline zeolite ZSM-5 and method of preparing the same, In: corporation MO, (editor). United States Patent Office. United States, 1967.
[21] S. Hong, Y. Uh, S. Woo, J. Lee, Thermal stability of [B]ZSM-5 molecular sieve, Korean J. Chem. Eng. 8 (1991) 1–5.
[22] J.L. Tallon, R.G. Buckley, O.F. THERMAL-DECOMPOSITION, The zeolite catalyst ZSM-5, J. Phys. Chem. 91 (1987) 1469–1475.
[23] G.T. Kokotailo, S.L. Lawton, D.H. Olson, W.M. Meier, Structure of synthetic zeolite ZSM-5, Nature 272 (1978) 437–438.
[24] S.Y. Sang, F.X. Chang, Z.M. Liu, C.Q. He, Y.L. He, L. Xu, Difference of ZSM-5 zeolites synthesized with various templates, Catal. Today 93–5 (2004) 729–734.
[25] J. Sebastian, S.A. Peter, R.V. Jasra, Adsorption of nitrogen, oxygen, and argon in cobalt(II)-exchanged zeolite X, Langmuir 21 (2005) 11220–11225.
[26] F.E. Trigueiro, D.F.J. Monteiro, F.M.Z. Zotin, E.F. Sousa-Aguiar, Thermal stability of Y zeolites containing different rare earth cations, J. Alloy Compd. 344 (2002) 337–341.
[27] K.S.W. Sing, D.H. Everett, R.A.W. Haul, L. Moscou, R.A. Pierotti, J. Rouquerol, et al., Reporting physisorption data for gas solid systems with special reference to the determination of surface-area and porosity (RECOMMENDATIONS 1984), Pure Appl. Chem. 57 (1985) 603–619.
[28] Y.-S. Bae, A.Ö. Yazaydın, R.Q. Snurr, Evaluation of the BET Method for determining surface areas of MOFs and zeolites that contain ultra-micropores, Langmuir 26 (2010) 5475–5483.
[29] S. Brunauer, P.H. Emmett, E. Teller, Adsorption of gases in multimolecular layers, J. Am. Chem. Soc. 60 (1938) 309–319.
[30] P.M. Jardim, B.A. Marinkovic, A. Saavedra, L.Y. Lau, C. Baehtz, F. Rizzo, A comparison between thermal expansion properties of hydrated and dehydrated orthorhombic HZSM-5 zeolite, Microporous Mesoporous Mater. 76 (2004) 23–28.
[31] W. Song, R.E. Justice, C.A. Jones, V.H. Grassian, S.C. Larsen, Synthesis, characterization, and adsorption properties of nanocrystalline ZSM-5, Langmuir 20 (2004) 8301–8306.
[32] T.A.J. Hardenberg, L. Mertens, P. Mesman, H.C. Muller, C.P. Nicolaides, A catalytic method for the quantitative-evaluation of crystallinities of ZSM-5 zeolite preparations, Zeolites 12 (1992) 685–689.
[33] M. Santhosh Kumar, A. Holmen, D. Chen, The influence of pore geometry of Pt containing ZSM-5, Beta and SBA-15 catalysts on dehydrogenation of propane, Microporous Mesoporous Mater. 126 (2009) 152–158.
[34] J.I. Villegas, N. Kumar, T. Heikkilä, V.P. Lehto, T. Salmi, D.Y. Murzin, Isomerization of n-butane to isobutane over Pt-modified Beta and ZSM-5 zeolite catalysts: catalyst deactivation and regeneration, Chem. Eng. J. 120 (2006) 83–89.
[35] K. Sing, The use of nitrogen adsorption for the characterisation of porous materials, Colloids Surf. A: Physicochem. Eng. Asp. 187–188 (2001) 3–9.
[36] W.M.C. Conner, Analyses of (AD)-Sorption for the estimation of pore-network dimensions and structure, J. Porous Mater. 2 (1995) 191–199.
[37] K.S.W. Sing, Adsorption methods for the characterization of porous materials, Adv. Colloid Interface Sci. 76–77 (1998) 3–11.
[38] WW, Russel. The Adsorption of Gases and Vapors. Volume I: Physical Adsorption (Brunauer, Stephen), Journal of Chemical Education, 1944, 21, 52.
[39] KSW Sing, Characterization of porous materials: past, present and future, Colloids Surf. A: Physicochem. Eng. Asp. 241 (2004) 3–7.
[40] M. Thommes, Physical Adsorption characterization of nanoporous materials, Chem. Ing. Tech. 82 (2010) 1059–1073.
[41] S.-H. Wu, C.-C. Hsieh, C.-C. Chiang, J.-J. Horng, W.-P. Pan, C.-M. Shu, Thermal analyses of home-made zeolite by DSC and TG, J. Therm. Anal. Calorim. 109 (2012) 945–950.
[42] A.K. Aboulgheit, M.A. Alhajjaji, A.M. Summan, S.M. Abdelhamid, Differential scanning calorimetry leads to high-precision for water in zeolites determined by thermogravimetry, Thermochim. Acta 126 (1988) 397–402.
[43] S. Matteucci, Y. Yampolskii, B.D. Freeman, I. Pinnau, Transport of gases and vapors in glassy and rubbery polymers, Mater. Sci. Membr. Gas. Vap. Sep. 1 (2006) 47.
[44] John W. Anthony RAB, Kenneth W. Bladh, Monte c. Nichols, Handbook of Mineralogy, VA 20151–1110, Mineralogical Society of America, Chantilly, USA, 2001.
[45] S. Arrhenius, On the reaction rate of the inversion of non-refined sugar upon souring, Z. Phys. Chem. 4 (1889) 226–248.